DETERMINATION OF THE AXIAL VECTOR FORM FACTOR IN THE RADIATIVE DECAY OF THE PION*†

A. Stetz, J. Carroll, N. Chirapatpimol‡,
M. Dixit‡, G. Igo‡, M. Nasser‡,
D. Ortendahl and V. Perez-Mendez

Lawrence Berkeley Laboratory
University of California
Berkeley, California

May, 1973

ABSTRACT

We report preliminary results on a measurement of the radiative decay of the pion, $\pi \rightarrow e\nu\gamma$. We use a magnet-spark chamber spectrometer system and a 24-element hodoscope of leadglass Cerenkov detectors to obtain positron momentum and positron-photon opening angle distributions. Using the theoretical distributions for the inner bremsstrahlung and the structure-dependent vector terms we can extract the axial vector contribution from our data. On the basis of 110 events we find the ratio of the axial vector to vector form factors, $\gamma = 0.11 \pm 0.07$.

---

* This work is supported by the United States Atomic Energy Commission.

† Invited paper given at the Symposium of the Division of Nuclear Physics, Washington, April, 1973.

‡ University of California, Los Angeles.

I. Introduction

The branching ratio for radiative pion decay, $\pi \rightarrow e\nu\gamma$, was first measured at CERN over ten years ago[1] in the hope of learning something about the intermediate vector boson. The results were inconclusive so far as the W was concerned, and the experiment was not repeated. Subsequent theoretical developments, however, such as quark models, the partially conserved axial vector current hypotehsis, and current algebra have resulted in definite predictions for the axial vector component, which can be compared with experiment. Since these theories involve detailed assumptions about the structure of weak interactions and since predictions based on different theories differ substantially, we can definitely rule out a number of hypotheses by determining the axial vector form factor in this decay.

To see why the radiative decay is a good reaction to explore the details of weak interactions, we recall that the ordinary decays of the pion, $\pi \rightarrow \mu\nu$ and $\pi \rightarrow e\nu$, in addition to being pure axial vector transitions, are bound by a sort of helicity selection rule which suppresses the electron mode by a factor of 10^4 relative to the muon mode. Both the helicity selection rule and the restriction to a pure axial vector transition are greatly relaxed if the pion decay goes via intermediate states which can emit a γ ray. This is not true of the bremsstrahlung component, which is still suppressed. Thus in the radiative decay we see the full complexity of the weak interactions without the constraints of ordinary selection rules and without an overwhelming background of bremsstrahlung.

The basic diagrams are shown in fig. 1. The internal bremsstrahlung (IB) arises from the two diagrams of fig. 1a in which a photon is radiated from one of the charged, external lines of the ordinary decay, $\pi \to e\nu$. Only the A (axial vector) interaction contributes. The rate of this process can be computed to first order of perturbation theory for the electromagnetic interactions if we know the rate for $\pi \to e\nu$. Then from Low's theorem the result is correct to zero order in the photon momentum. In this sense the bremsstrahlung contribution is trivial and tells us nothing about the interactions which is not already contained in the rate for $\pi \to e\nu$.

The interesting effect, fig. 1b, is a structure dependent (SD) process involving intermediate states generated by strong interactions or possibly by the W. Both V and A can contribute; moreover, there is interference between the SD and IB amplitudes. Our ignorance about the intermediate states can be collected into two form factors (there are no pseudoscalar or tensor terms as in nucleon beta decay), and since the momentum transfer is limited by half the pi mass the form factors can be approximated by constants. The vector part can be calculated from the rate for $\pi^0 \to \gamma\gamma$ using the conserved vector current hypothesis,[2] which gives a prescription for relating $\Delta I = 1$ electromagnetic transitions like π^0 decay to weak vector interactions in which one of the photons is replaced by a lepton pair. This leaves only one unknown, the axial vector form factor. This is <u>not</u> the same axial vector term which one measures in ordinary π decay. The extra photon gives rise to a whole new set of intermediate states, and it is these which we are trying to

investigate. Finally, it is customary to write the formula for the rates as a function of the ratio of the axial vector to vector form factors, usually called γ. The object of the experiment, then, is ultimately to measure γ.

II. Theoretical Predictions.

Recent Theoretical work on radiaitve decay is summarized below:

	Technique	Prediction
Kummer & Kuti[3]	Quark Model	$\|\gamma\| = 0$
Das, Mathur, and Okubo[4]	Current Algebra Soft Pion Approximation	$\|\gamma\| = 0.48$
Vaishya[5]	Current Algebra Hard Pion Techniques	$\|\gamma\| = 0.24$
Berezinskii	Current Algebra Hard Pion Techniques	$\|\gamma\| = 1.75$

The static quark model yields an unambiguous prediction: besides the internal bremsstrahlung, all other intrinsic strong axial vector contributions cancel. This result is independent of the free parameters that appear in quark models, and can be taken as a "theorem" of the static quark model or SU(6).

The other predictions are all based on current algebra and the PCAC hypothesis. Das, Mathur, and Okubo use the "soft pion" approximation in which the mass of the pion is taken as zero at one intermediate

step in the calculation. The last two papers circumvent the soft-pion approximation at the expense of introducing a free parameter that appears as a subtraction constant in their dispersion integrals. This free parameter, which is responsible for the disparity between the last two predictions, cannot be calculated a priori but can be related to other experimental parameters such as the width of the ρ, the rate for $A_1 \rightarrow \pi\rho$, and the charge radius of the π.[7]

III. Kinematics and Experimental Design.

In the case of a three-body decay with the initial particle at rest one must measure two independent kinematic quantities to completely determine the kinematics. The three variables that are experimentally accessible are the positron and photon momenta and their opening angle. It is more convenient, however, to use the variables x, y, and λ defined by

$$x = \frac{2P_\gamma}{m_\pi}$$

$$y = \frac{2P_e}{m_\pi}$$

$$\lambda = \mathrm{Sin}^2(\theta/2).$$

Conservation of momentum and energy yields one relation among these variables (we ignore the electron mass)

$$\lambda x y = x + y - 1.$$

This is plotted as a relationship between x and y for fixed θ in fig. 2.

In order to avoid various backgrounds and make our experiment as sensitive as possible to γ we confine ourselves to the upper right-hand corner of the plot. In this region the interference between SD and IB components is negligible and the IB contributes less than 30% to the total rate.

The differential rates are written most simply as functions of x and y. For the IB part

$$\frac{d^2W_{IB}}{dxdy} = \left| \frac{\alpha W_{e\nu}}{2\pi} \right| \left| \frac{1 - y}{x^2} \right| \frac{(x - 1)^2 + 1}{x + y - 1} \qquad (1)$$

where α is the fine-structure constant and $W_{e\nu}$ is the rate for $\pi \to e\nu$, 4.76×10^3 sec^{-1}. The SD part is given by

$$\frac{d^2W_{SD}}{dxdy} = \left(\frac{\alpha W_{e\nu}}{2\pi} \right) \left(\frac{m_\pi}{2m_e} \right)^2 h_2^2 \left[F(x,y)(1 + \gamma)^2 + G(x,y)(1 - \gamma)^2 \right]$$

$$F(x,y) = (1 - x)(x + y - 1)^2 \qquad (2)$$

$$G(x,y) = (1 - x)(1 - y)^2$$

m_e is the electron mass and h_2 is the vector form factor. We use the CVC value[2]

$$h_2^2 = \left(\frac{1}{4\pi}\right)^2 \left(\frac{G_V^2 m_\pi^4}{\alpha^2}\right) \left(\frac{2m_e}{m_\pi}\right)^2 \frac{W_{\pi^0}}{W_{e\nu}} \qquad (3)$$

where G_V is the weak interaction coupling constant and W_{π^0} is the rate for $\pi^0 \to \gamma\gamma$. Using the most recent value for the π^0 lifetime,[8] $\tau_{\pi^0} = 0.56 \times 10^{-16}$ sec we get $h_2^2 = 1.12 \times 10^{-3}$. The integrated rates $\frac{dW}{dy}$ and $\frac{dW}{d\theta}$ are shown in fig. 3-6. Evidently the IB distributions favor small opening angles and low photon energies whereas the SD component has its maximum sensitivity to γ in a region which is not obscured by bremsstrahlung.

In this kinematic region the function $G(x,y)$ defined above is only about 5% of $F(x,y)$. As a consequence the distributions do not change much under the replacement $\gamma \to -\gamma - 2$. With sufficient statistics and resolution this ambiguity can be resolved by taking advantage of the correlations in energy and angle, which are quite different in F and G.

The only published experiment on radiative decay was done by Depommier, Heintze, Rubbia, and Soergel at CERN about 10 years ago.[1] They simply measured the energies of wide-angle positron-photon pairs using a NaI crystal for the positron and a leadglass Cerenkov counter for the photon. No attempt was made to measure the opening angle beyond the limits imposed by the apparatus. On the basis of 143 events they observed a branching ratio of 3×10^{-8} into a kinematic region defined by E_γ and $E_e \geq$ 50 MeV. (Since the bremsstrahlung component diverges at small photon energies the notion of a "total branching ratio" is not

very meaningful.) Using the latest value for the π^o lifetime[8] they obtained a value of γ "consistent with zero". (No error quoted.) Their resolution was not sufficient to rule out the complementary value $\gamma = -2$, however.

IV. Experimental Layout.

Since the experiment was not repeated we decided to redo it in an attempt to achieve better statistics, obtain an opening angle distribution, and eliminate the two-fold ambiguity in γ. The layout is shown in fig. 7.

Our beam is a large solid angle, low-energy, acromatic pion beam. At maximum cyclotron intensity we stop $\sim 1/4 \times 10^6$ π^+/sec, and we could easily use another factor of four in intensity. The beam actually consists predominately of positrons with about 65% e^+, 30% π^+ and 5% muons. The pions are stopped in a counter hodoscope, which is slanted to increase the stopping material without degrading the positrons too much.

The positron momentum is measured in the magnet-spark chamber spectrometer system. Our resolution is about 2 MeV due to multiple scattering in the spark chambers and uncertainty in the energy deposited in the stopped. The momentum normalization and the resolution are determined by fitting the cut-off in the momentum spectrum of positrons from μ decay and by occasionally triggering the system on the mono-energetic electrons from $\pi^+ \rightarrow e^+ \nu$.

The photon is detected in a Cerenkov hodoscope consisting of 24 blocks of lead glass, each with its own 5 in. photomultiplier. The

counter is used to determine the position of the photon to within ± 8° and as a threshold device in the master trigger. Although we do not attempt to use the photon energy determined from its pulseheight we have measured the resolution of the counter in an electron beam at 50 MeV/c. The resolution was 20%; this is good for a Cerenkov counter at these energies, but not good enough to make a meaningful measurement for this reaction. Since our acceptance depends on the threshold we have taken pains to monitor the gain of each individual phototube with a calibrated light pulser and a system of fibre optic light-pipes, which steer the light into the various tubes. In the anlysis that follows we assume that the detection efficiency of this device is 100% for photons of interest. In reality, the efficiency is somewhat lower (~ 20 meV), but it will require a separate calibration experiment to determine this efficiency exactly.

Our stopping flux is determined in a straightforward way with a series of beam counters, the stopping hodoscope, and a final anti-counter. We need to know, however, what fraction of the stopped particles actually are pions. This is done by accumulating a spectrum of the time elapsed between the stopping of a beam particle and the detection of a decay positron. A representative spectrum is shown in fig. 8. Since most of these positrons result from a two-step process

$$\pi^+ \rightarrow \mu^+ + \nu$$
$$\hookrightarrow \quad e^+ + \nu + \bar{\nu}$$

the curve is a parent-daughter distribution. The contamination of stopped μ's can be determined by extrapolating the curve under the small "prompt" peak to T = 0 and subtracting the flat background that appears at negative T. In this way we conclude that our stopping flux is 95 ± 2% pions.

V. Results.

Since our experiment measures no redundant kinematic information we need an extra parameter to distinguish the radiative decay events from the background. Since the background consists of uncorrelated events in the Cerenkov counter and spectrometer system we can measure the time difference, ΔT, between the $\check{C}$ pulse and the e^+ trigger. The radiative decay events should stand out as a sharp peak at $\Delta T = 0$ above a flat background. A sample of our data is shown in fig. 9. This represents about half of what we hope will be our final data. The background subtraction is unambiguous and amounts to about 20% of the events under the peak. After all cuts have been imposed on the data and the background subtracted we are left with 110 events.

One can get an impression of the quality of this data by plotting a decay time distribution. Fig. 10 shows a histogram of the time elapsed between the stopping of a beam particle and the detection of a $e^+ - \gamma$ coincidence. The smooth curve is the pion decay curve normalized to the total number of events in the histogram. There is no apparent contamination here, either from the three-step reaction

$$\pi^+ n \rightarrow \pi^o P$$
$$\pi^o \rightarrow \gamma\gamma$$
$$\gamma \rightarrow e^+ e^-$$

which was a troublesome source of background for the original experiment, or from accidental coincidences with μ decay.

Figure 11 shows the data in the momentum projection weighted by the acceptance of the apparatus. The smooth curve is a theoretical distribution with the experimental resolution folded in. It assumes a π^o lifetime of 0.56×10^{-16} sec [8] and $\gamma = 0.11$. This value for γ was calculated from the number of events observed; no attempt has been made to fit the observed distributions. The statistical error on γ is $\pm$ 0.07. Figure 12 shows the data as a function of the opening angle. The smooth curve corresponds to $\gamma = 0.11$, but at this stage we are unable to rule out the complementary value $\gamma = -2.1$. We expect to be able to resolve the ambiguity by fitting the data in p and θ simultaneously.

In order to find γ we must assume a value for the π^o lifetime (to get W_{π^o} in equation 3). In this report we have assumed a value of 0.56×10^{-16} sec. [8] in order to consistently compare the previous experiment, the theoretical predictions, and our results. We have no reason, however, to favor this result over several other recent measurements of the π^o lifetime, and this uncertainty seriously undermines our results as seen in fig. 13. In this graph the value of γ calculated from our data is plotted against the assumed value for the π^o lifetime. The six data points represent the six most recent measurements of the lifetime.

The horizontal error bars are the errors assigned by the original authors to their results. The vertical error bars are our statistical error. Even with 110 events this error is much less than the uncertainty generated by our misgivings about the π^o lifetime. We can only hope that with the energy and consequently the time dilation available at N.A.L., the lifetime of the π^o will eventually be determined in a definitive way.

VI. Conclusion

We have measured the branching ratio of the radiative decay, $\pi \to e\nu\gamma$. Assuming a π^o lifetime of 0.56×10^{-16} sec we have obtained $\gamma = 0.11 \pm 0.07$, which is consistent with the earlier result of Depommier, et. al. At the present time we are unable to rule out the complementary value $\gamma = -2.1$. Although no final comparison with theory can be made until this ambiguity is resolved and the π^o lifetime question is settled, our results suggest that γ is very close to zero in agreement with the static quark model.

REFERENCES

1. P. Depommier, J. Heintze, C. Rubbia, and V. Soergel, Physics Letters 7 (1963) 285; also V. Soergel, Proceedings of the SIN Summer School, Leysin, 1969.

2. V. F. Müller, Zeitschrift für Physik 173 (1963) 438.

3. W. Kummer and J. Kuti, Nuovo Cimento 45 (1966) 242.

4. T. Das, V. S. Mathur, and S. Okubo, Physical Review Letters 19 (1967) 859. The original published value was $|\gamma| = 0.6$ but this depends on the π^0 lifetime assumed in the calculations. Since various values have been used in the literature we have recalculated the results of ref. 4, 5, and 6 assuming $\tau_{\pi^0} = 0.56 \times 10^{-16}$ sec. This makes the predictions consistent with our work and Soergel's article in the SIN Proceedings (ref. 1), but not with the original paper of Depommier, Heintze, Rubbia and Soergel.

5. J. S. Vaishya, Physical Review 173 (1968) 1757.

6. V. S. Berezinskii, Soviet Journal of Nuclear Physics 8 (1969) 700.

7. R. E. Marshak, Riazzuddin, and C. P. Ryan, Theory of Weak Interactions in Particle Physics, New York, Wiley-Interscience (1969).

8. G. Bellettini, C. Bemporad, P. L. Braccini, C. Bradaschia, and L. Foa, Nuovo Cimento 66A (1970) 243.

FIGURE CAPTIONS

Fig. 1. (a) Internal bremsstrahlung diagrams.
(b) Structure dependent diagram.

Fig. 2 Kinematics for $\pi \to e\nu\gamma$. The curves show relationship between x and y for fixed values of the opening angle.

Fig. 3 Bremsstrahlung rate as a function of positron momentum. The sharp cusp is a result of the kinematic boundaries over which the angular integration is performed. At maximum positron momentum the lower limit of this integral is due to the angular cutoff of our apparatus. At smaller positron momenta this limit is imposed by the threshold requirement on photon energy.

The units of $\frac{dW}{dy}$ are branching ratio $\times 10^{10}$ per MeV here and in fig. 5.

Fig. 4 Bremsstrahlung rate as a function of opening angle.

The units of $\frac{dW}{d\theta}$ are branching ratio $\times 10^{10}$ per degree here and in fig. 6.

Fig. 5 Structure dependent rate as a function of positron momentum for various values of γ.

Fig. 6 Structure dependent rate as a function of opening angle for various values of γ.

Fig. 7 Experimental layout.

Fig. 8 Elapsed time spectrum for determining muon contamination in beam.

Fig. 9 Spectrum of time differences, ΔT, between positron and photon signals.

Fig. 10 Decay time distribution. The smooth curve is pion decay exponential normalized to the total number of events in histogram.

Fig. 11 Positron momentum spectrum. Histogram consists of events weighted by experimental acceptance. The curve is the theoretical distribution for $\gamma = 0.1$ with the experimental resolution folded in.

Fig. 12 Opening angle distribution. The curve has the same significance as in fig. 11.

Fig. 13 Relationship between γ and the assumed value of the π^0 lifetime. The data points are the six most recent measurements of the lifetime.

Internal Bremsstrahlung

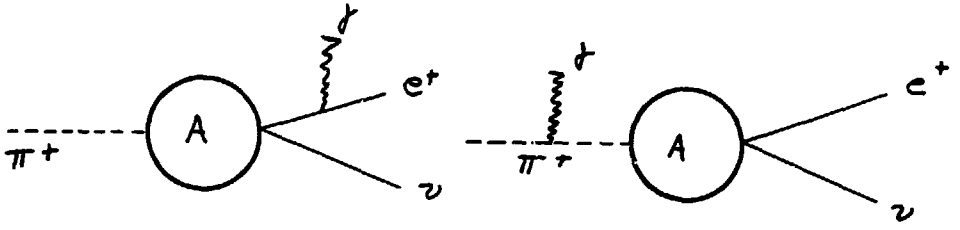

Structure Dependent Effect

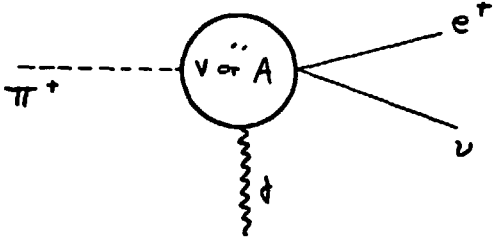

XBL 735-531

Fig. 1

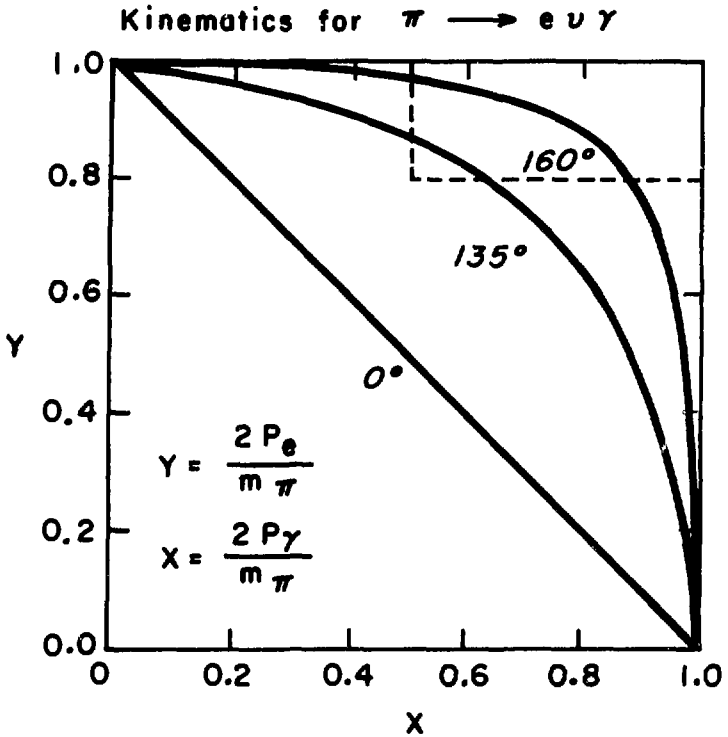
Kinematics for π ⟶ e υ γ
1.0
0.8
0.6
0.4
0.2
0.0
Y
0
0.2
0.4
0.6
0.8
1.0
X
160°
135°
0°
Y = 2 Pe / m π
X = 2 Pγ / m π
XBL733-2574

Fig. 2

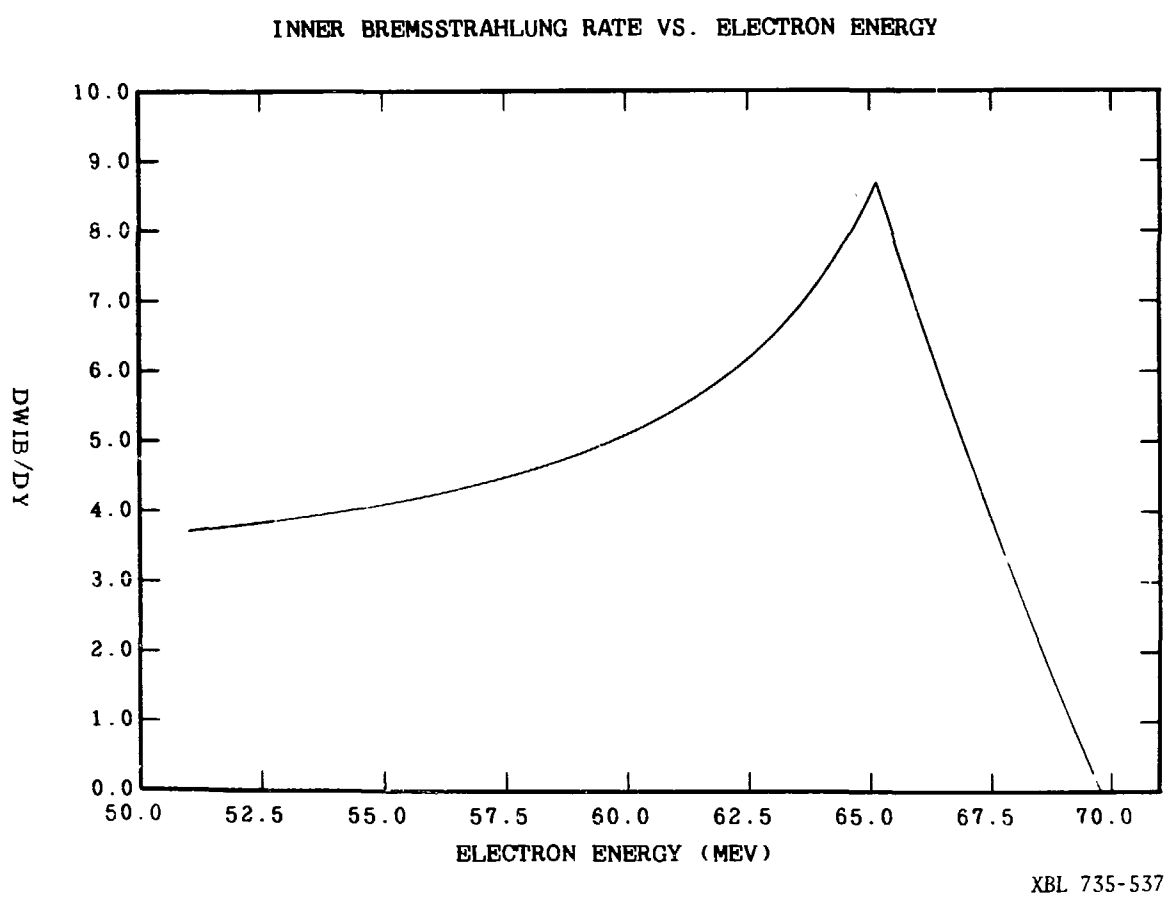
INNER BREMSSTRAHLUNG RATE VS. ELECTRON ENERGY
DWIB/DY
10.0
9.0
8.0
7.0
6.0
5.0
4.0
3.0
2.0
1.0
0.0
50.0
52.5
55.0
57.5
60.0
62.5
65.0
67.5
70.0
ELECTRON ENERGY (MEV)
XBL 735-537

Fig. 3

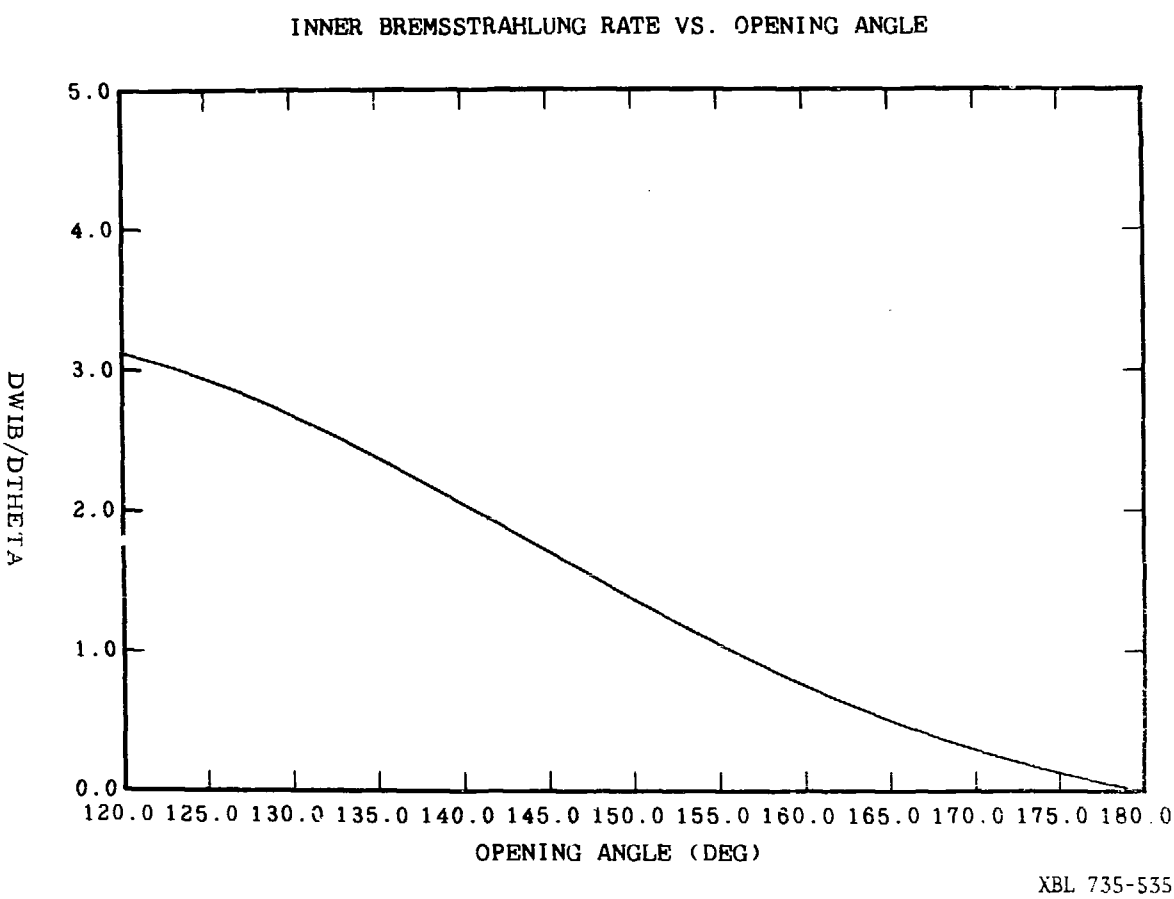
INNER BREMSSTRAHLUNG RATE VS. OPENING ANGLE
DWIB/DTHETA
5.0
4.0
3.0
2.0
1.0
0.0
120.0 125.0 130.0 135.0 140.0 145.0 150.0 155.0 160.0 165.0 170.0 175.0 180.0
OPENING ANGLE (DEG)
XBL 735-535

Fig. 4

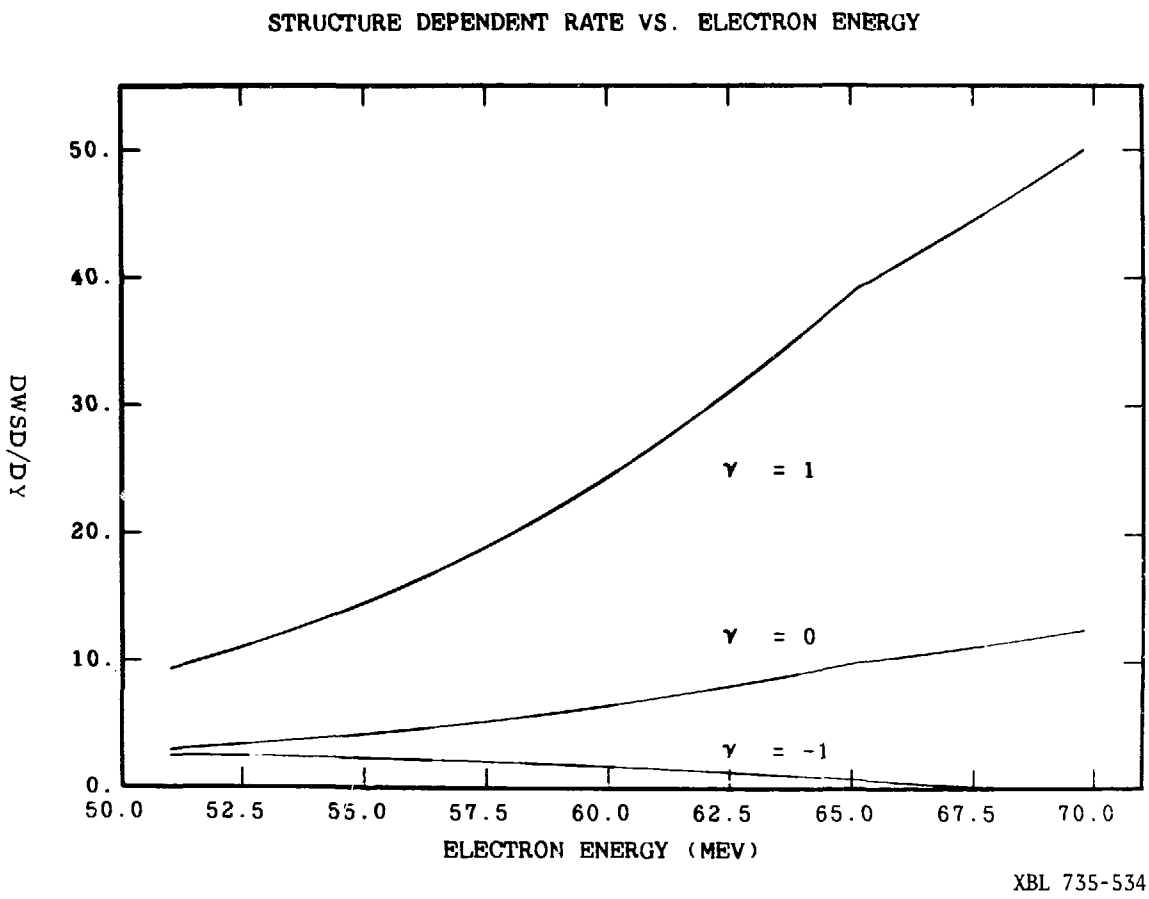
STRUCTURE DEPENDENT RATE VS. ELECTRON ENERGY
DWSD/DY
50.
40.
30.
20.
10.
0.
50.0
52.5
55.0
57.5
60.0
62.5
65.0
67.5
70.0
ELECTRON ENERGY (MEV)
γ = 1
γ = 0
γ = -1
XBL 735-534

Fig. 5

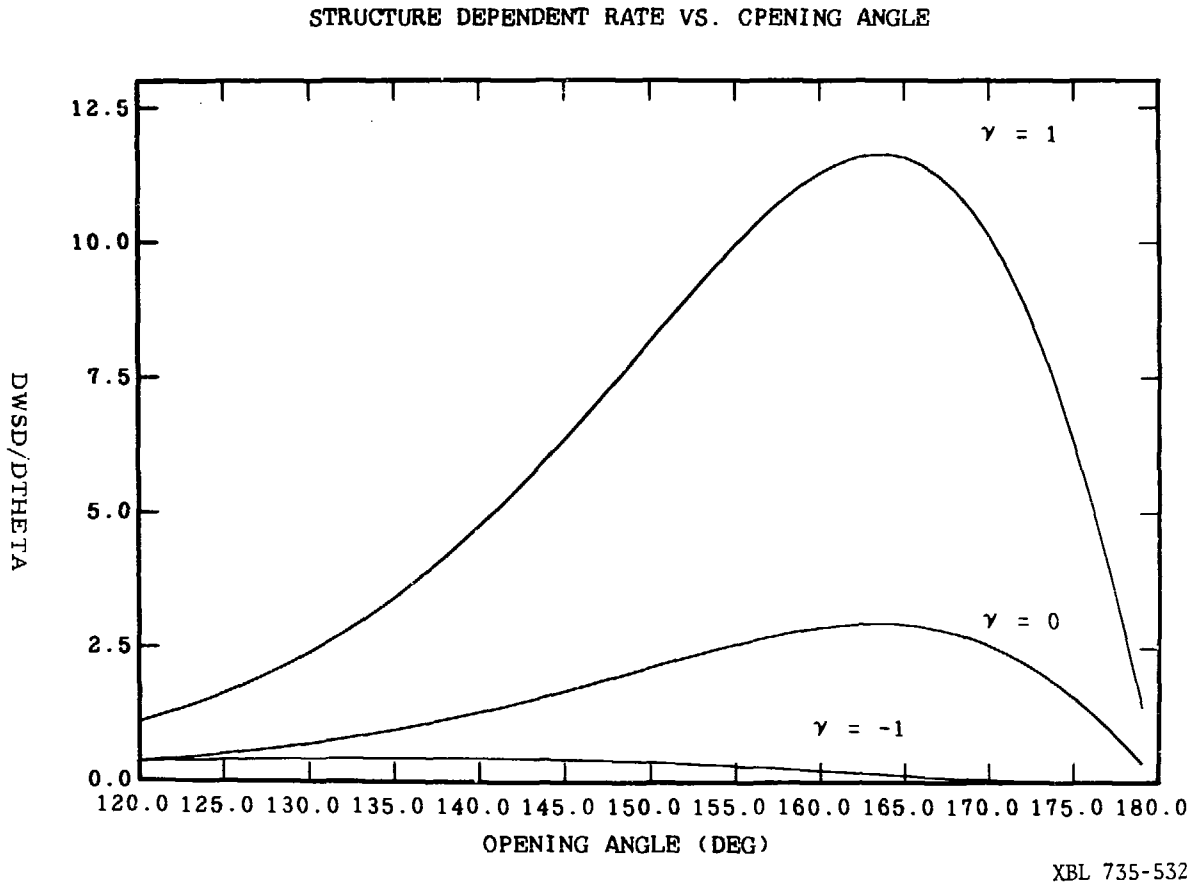
STRUCTURE DEPENDENT RATE VS. OPENING ANGLE
DWSD/DTHETA
12.5
10.0
7.5
5.0
2.5
0.0
γ = 1
γ = 0
γ = -1
120.0 125.0 130.0 135.0 140.0 145.0 150.0 155.0 160.0 165.0 170.0 175.0 180.0
OPENING ANGLE (DEG)
XBL 735-532

Fig. 6

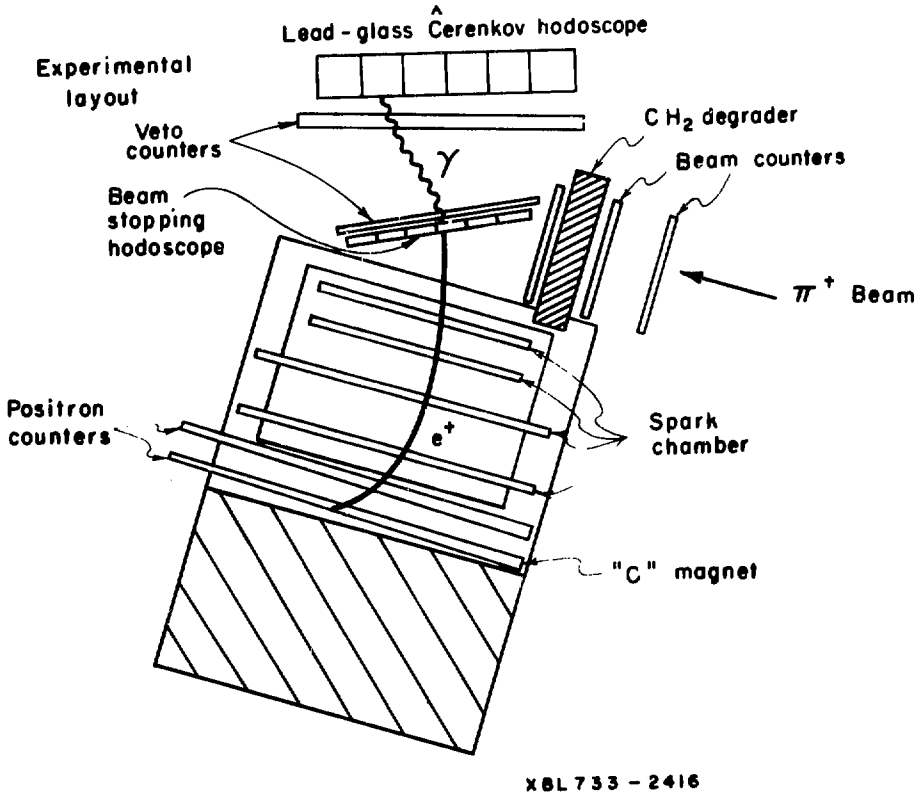
Lead - glass Cerenkov hodoscope
Experimental layout
Veto counters
γ
C H2 degrader
Beam counters
Beam stopping hodoscope
π+ Beam
Positron counters
e+
Spark chamber
"C" magnet
XBL733 - 2416

Fig. 7

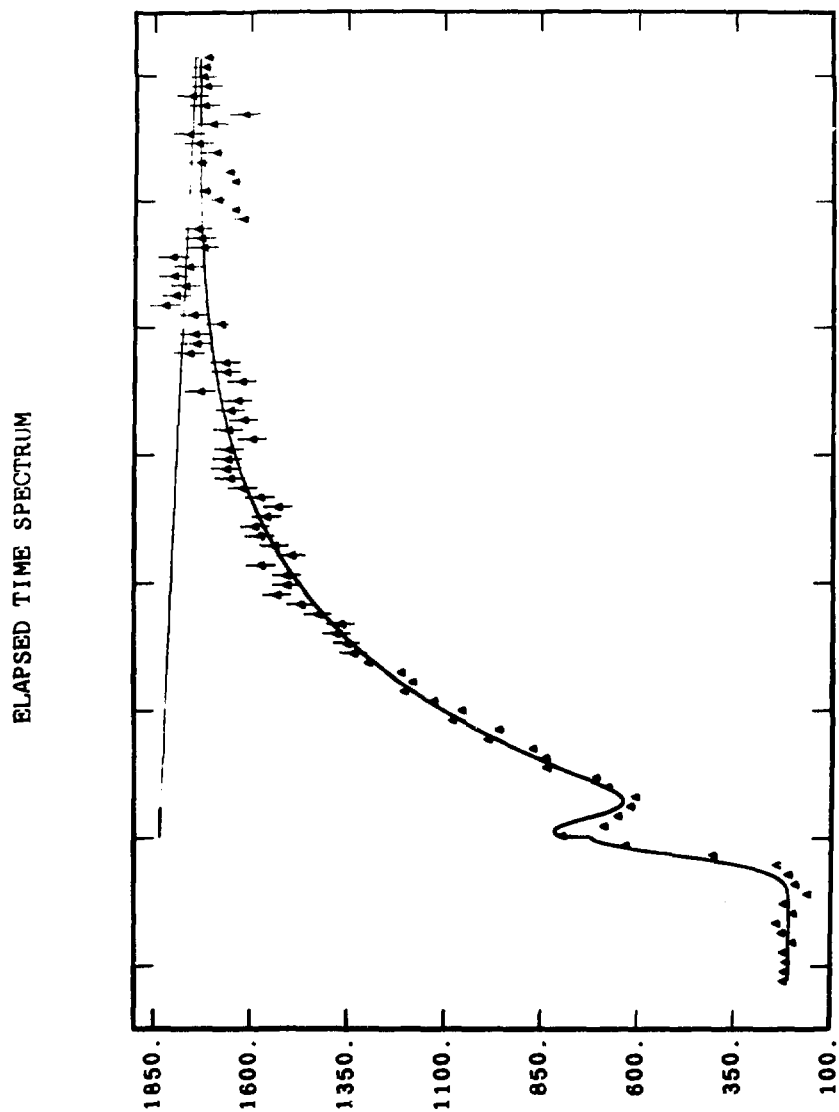
ELAPSED TIME SPECTRUM
COUNTS PER 1.5 NS
1850.
1600.
1350.
1100.
850.
600.
350.
100.
-20.
0.
20.
40.
60.
80.
100.
120.
ELAPSED TIME (NS)
XBL 735-533

Fig. 8

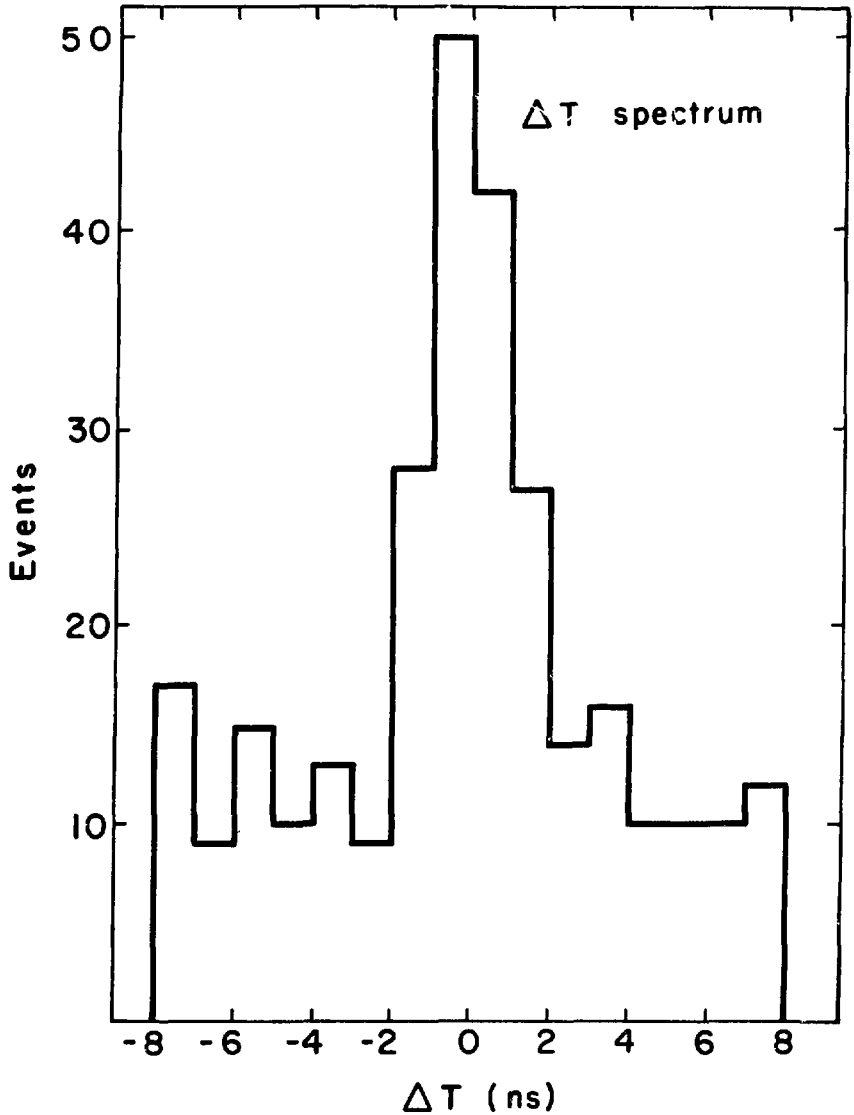

XBL733-2575

Fig. 9

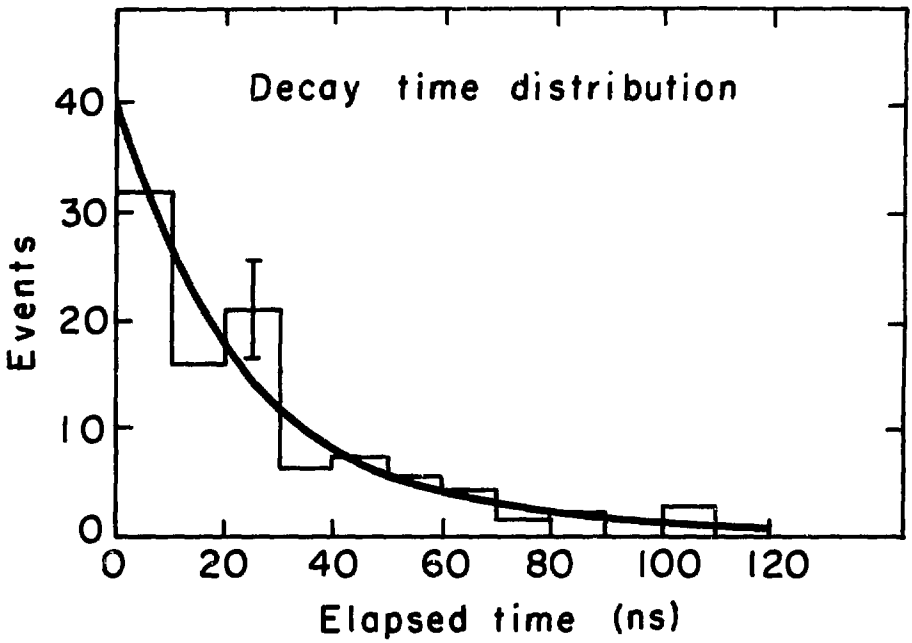

XBL733-2576

Fig. 10

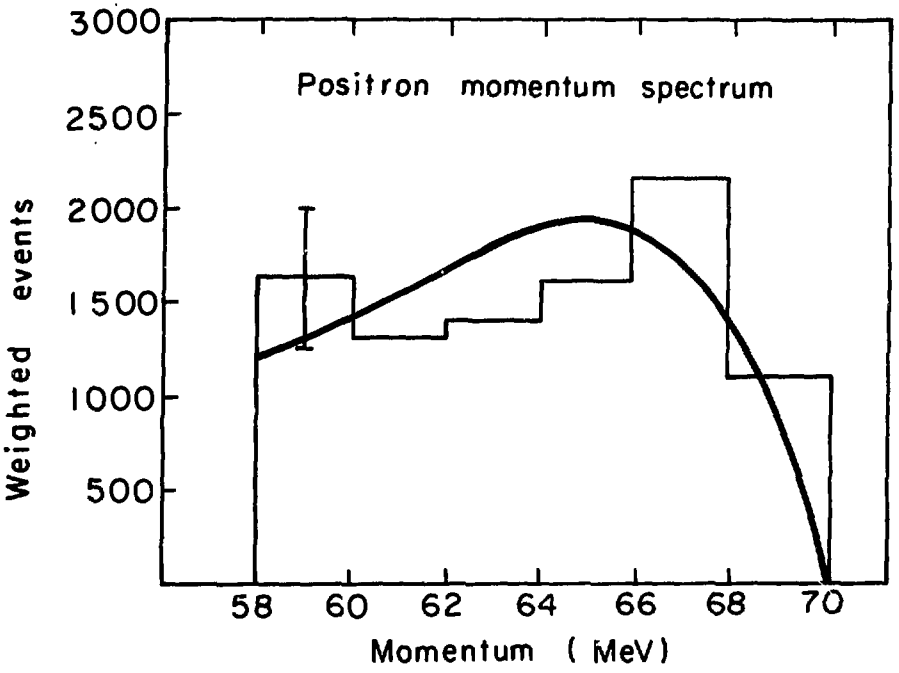

XBL733-2578

Fig. 11

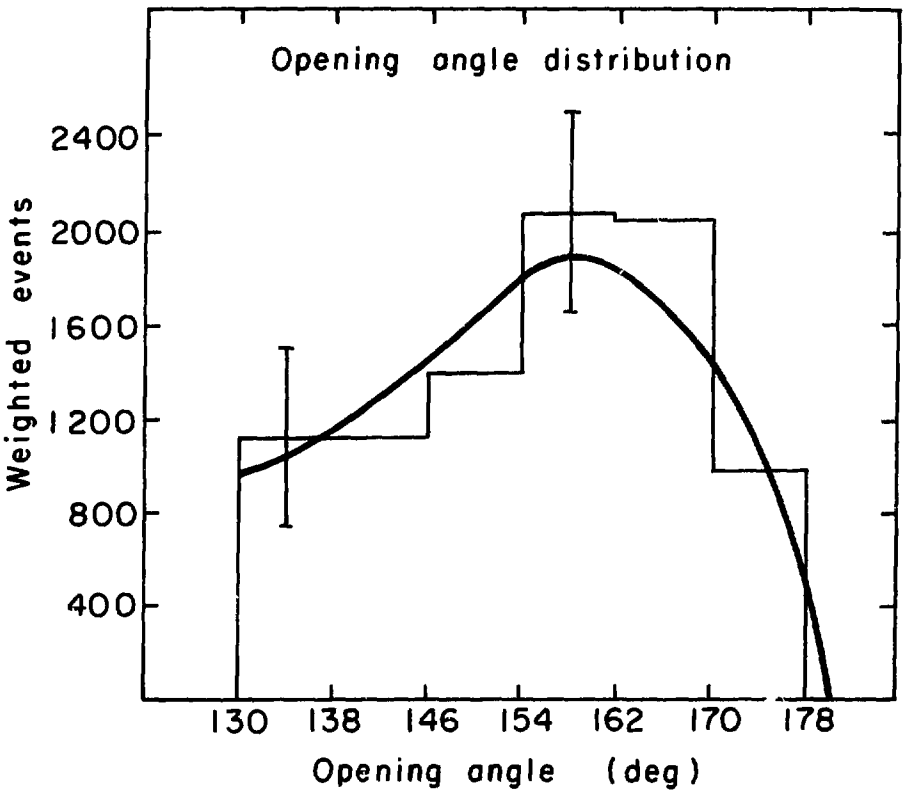

XBL733-2577

Fig. 12

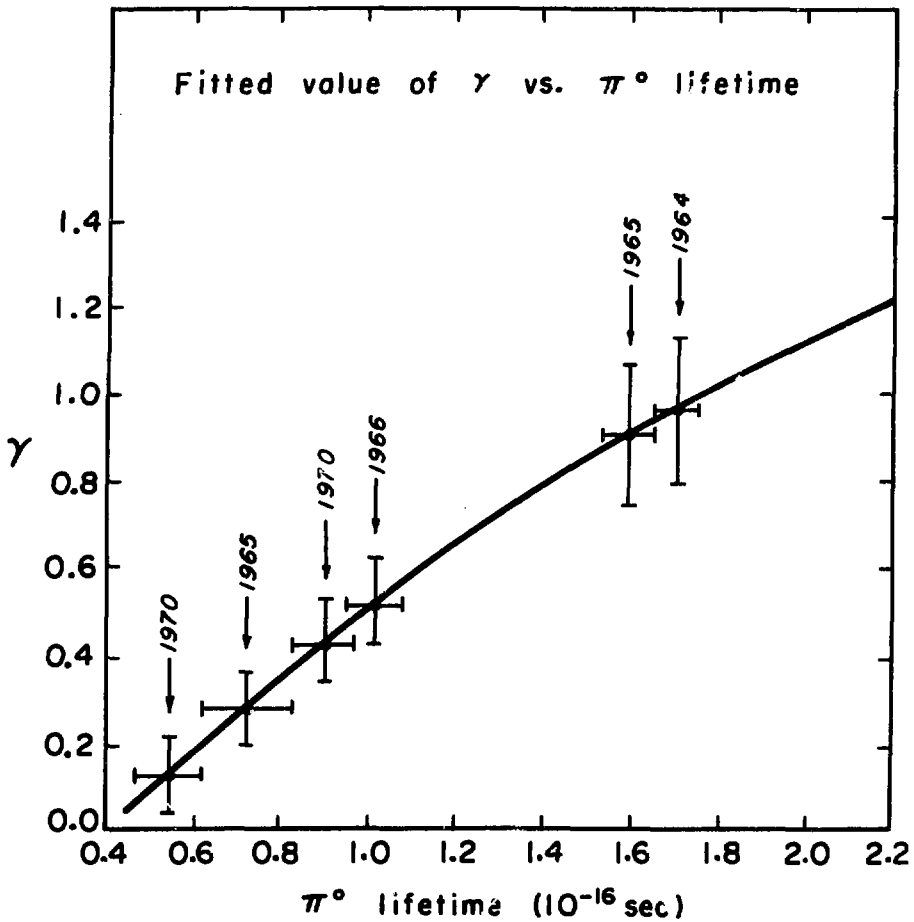

XBL733-2573

Fig. 13